

ISTITUTO NAZIONALE DI RICERCA METROLOGICA  
Repository Istituzionale

3D printable light-responsive polymers

This is the author's accepted version of the contribution published as:

*Original*

3D printable light-responsive polymers / Roppolo, I.; Chiappone, A.; Angelini, A.; Stassi, S.; Frascella, F.; Pirri, C. F.; Ricciardi, C.; Descrovi, E.. - In: MATERIALS HORIZONS. - ISSN 2051-6347. - 4:3(2017), pp. 396-401.  
[10.1039/c7mh00072c]

*Availability:*

This version is available at: 11696/63072 since: 2021-01-04T13:22:58Z

*Publisher:*

Royal Society of Chemistry

*Published*

DOI:10.1039/c7mh00072c

*Terms of use:*

Visibile a tutti

This article is made available under terms and conditions as specified in the corresponding bibliographic description in the repository

*Publisher copyright*

(Article begins on next page)



Journal Name

COMMUNICATION

### 3D printable light-responsive polymers

I. Roppolo,<sup>a†</sup> A. Chiappone,<sup>a</sup> A. Angelini,<sup>b</sup> S. Stassi,<sup>b</sup> F. Frascella,<sup>b</sup> C. F. Pirri,<sup>ab</sup> C. Ricciardi,<sup>b</sup> E. Descrovi<sup>b†</sup>

Received 00th January 20xx,  
Accepted 00th January 20xx

DOI: 10.1039/x0xx00000x

www.rsc.org/

**New photo-curable polymers for 3D printing are provided, exhibiting mechanical light-responsivity upon laser irradiation. Azobenzene moieties are employed both as dyes in the 3D printing process and as active groups providing the desired light responsivity. The incorporation of azobenzene units into polymeric matrices allows a reversible and controllable change of the Young's modulus of a crosslinked micrometric structure. Depending on the temperature of operation, laser irradiation induces either a decrease (photo-softening) or an increase (photo-hardening) of the Young's modulus. Such a behaviour can be spatially controlled in order to locally modify the mechanical features of 3D printed objects such as microcantilevers.**

3D printing is an emerging field, which gains year after year more and more importance both in scientific and industrial frameworks.<sup>1</sup> Relevant applications span from aerospace<sup>2, 3</sup> to biomedical engineering<sup>4, 5</sup> passing through electronics,<sup>6, 7</sup> mechanics<sup>8-10</sup> and many other domains.<sup>11-13</sup> Among the different materials that could be 3D-printed, a prominent role is played by polymers, which cover the largest part of the market.<sup>14</sup> After the development of the first stereolithographic apparatus (SLA) in the '80s, different techniques have been developed, involving the use of polymeric materials in different forms, namely wires or pastes (Fused Deposition Modeling – FDM), powders (Selective Laser Sintering – SLS) or photocurable formulations (SLA and its evolution Digital Light Processing – DLP). Each of these techniques presents advantages and drawbacks, as largely reported in literature,<sup>15</sup> in particular light-based technologies are known for being the fastest and most

precise, even if they suffer of a limited range of available printable materials. However, in the frame of developing functional materials, they are generally preferred, because operating with liquid formulations offers the possibility to easily modify and tailor materials' properties for providing new functionalities.<sup>16-18</sup>

All SLA and DLP techniques are based on the use of a digital model file (CAD) of the object that has to be printed. Such a digital object is then sliced, each slice containing the set of points to be irradiated by a light source incident on the vat containing the photocurable formulation. The main difference between these two techniques consists in the fact that SLA involves a point-by-point exposure while in DLP the whole layer is exposed contemporarily, resulting in a faster printing process. The illuminated points undergo solidification through photopolymerization.<sup>19</sup> In this way, the structure is built layer by layer, finally resulting in a solid 3D object.<sup>20</sup> There are three main ingredients in a photocurable formulation for 3D printing: the monomers/oligomers, which will form the polymeric structure; a photoinitiator, for initiating the photopolymerization process, and a light absorber, typically a dye.<sup>21</sup> The dye is used to improve the light spatial confinement within the curable formulation, in order to avoid undesired over-curing and a loss of spatial resolution during the printing process.<sup>22</sup> No additional features are generally requested to the dye, whose residual effect is just a final coloring of the object.<sup>23</sup> When some given functionality is desired on the final 3D printed object, a tailoring of the photocurable formulation is required, typically adding fillers.<sup>20</sup>

In this work we propose an alternative approach, whereby a light-responsive functionality is provided by the dye component. We introduce azobenzene compounds within photocurable polymeric formulations and achieve an accurate 3D printing of crosslinked matrices, whose mechanical properties can be reversibly tuned upon laser irradiation.

Azobenzene is a well-known photochromic chemical species,<sup>24</sup> i.e. a molecule able to undergo reversible transformation between two isomers with specific absorption spectra.<sup>25</sup> In

<sup>a</sup>Center for Sustainable Future Technology, Istituto Italiano di Tecnologia, Corso Trento 21, 10129 Torino, Italy.

<sup>b</sup>Dipartimento di Scienza Applicata e Tecnologia, Politecnico di Torino, C.so Duca degli Abruzzi 24, 10129 Torino, Italy.

†Corresponding Authors

E-mails: ignazio.roppolo@iit.it, emiliano.descrovi@polito.it

Electronic Supplementary Information (ESI) available: Photoreology measurements, UV-Vis performed on printed structures, mechanical test upon laser irradiation and microcantilever. See DOI: 10.1039/x0xx00000x

general, linear trans-Azobenzene molecule isomerizes into cis-form upon UV irradiation, resulting in an almost completely thermo-reversible change.<sup>26</sup> However, cyclic isomerization can

be obtained upon a continuous visible light irradiation.<sup>27</sup> In the recent years azo moieties have been used in polymer matrices

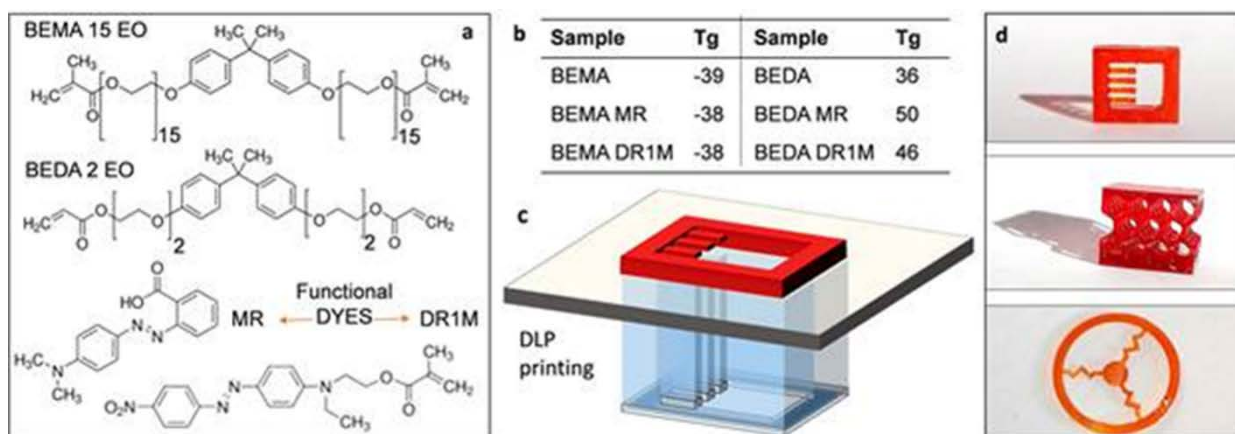


**Figure 1.** a) Monomers and dyes used in this work. b) List of the prepared samples and their  $T_g$ . c) Sketch of digital projection printing setup that projects dynamic digital masks on the photocurable formulation featuring the formation of the 3D structures. d) Examples of DLP 3D printed objects

both as un-linked dispersed moieties,<sup>26</sup> and as lateral pendant of a polymeric backbone<sup>28</sup> or constituting unit of polymer chains.<sup>29</sup> It has been largely reported that the use of azobenzene molecules in polymeric constructs can result in several light-triggered macroscopic effects, such as optical birefringence,<sup>30</sup> mass migration,<sup>31</sup> photofluidization,<sup>31, 32</sup> tuning of elastic modulus,<sup>33, 34</sup> or wettability a,b, phase separation,<sup>35</sup> whose underlying physical mechanisms are still unclear to some extent.<sup>36-38</sup> As opto-mechanical transduction is concerned, several strategies have been suggested for amplifying the nanoscopic force produced at each trans-cis isomerization of individual azobenzene molecules to a larger scale,<sup>39</sup> one of the most promising being based on a crosslinkable compound containing Liquid Crystal Elastomers (LCE).<sup>24</sup> However, due to pre-defined spatial alignment of LCE chains, the light-induced mechanical actuation provided by the azo component is suffering for strong anisotropy.<sup>40</sup> According to our approach, we provide a printed crosslinked amorphous network incorporating azopolymers that are nevertheless able to light-trigger relevant changes in the elastic modulus and isotropic reversible expansions/contractions over a macroscopic scale. Two monomers were considered for the production of DLP/SL 3D printable formulations, namely BEDA and BEMA, both containing a Bisphenol-A group and ethylene oxide chains (Figure 1a). The main difference between the two monomers is represented by the ethylene oxide chain length which is low in BEDA (2 EO/phenol) and relatively high in BEMA (15 EO/phenol). As a consequence, a large difference between the glass transition temperatures ( $T_g$ ) of the thermoset networks that the two monomers can generate after curing is produced.<sup>41</sup> BEDA forms a rigid network characterized by a  $T_g$  higher than room temperature, while BEMA results in a more loosely network with lower  $T_g$  (Figure 1, b). Methyl Red (MR) and dispersed red methacrylate (DR1M) were tested as light

responsive functional dyes;<sup>42</sup> the first one has been chosen since it can be easily embedded as a filler within the polymer network, whilst the second one, bearing a methacrylic group, can react with the monomers and therefore can be chemically linked to the network.

Before printing, the reactivity of the formulations containing the azobenzene-based dyes was investigated performing photorheology tests (see ESI Figure S1). A significant change of the elastic and viscous modulus is observed during photocuring of the curable formulations. Such variations is faster for BEDA samples and slightly slower for BEMA due to the slower polymerization kinetics of the methacrylate monomers.<sup>41</sup> For both monomers, the presence of the dyes slows down the start of the crosslinking reaction, as expected for colored formulations, thus causing some delay in the achievement of the gel point (when  $G' = G''$ ). The evaluation of the gel point gives an indication on how to balance the two adjustable printing parameters (i.e. layer thickness and exposure time). Nevertheless, the best values for printing are always empirically defined, on the basis of the printing accuracy. The limited delays in gelling time between neat formulations and formulations containing azobenzene molecules show that the azo-moieties do not hinder the monomers' photopolymerization and thus they could be effectively used as dyes for 3D printing process.

UV-visible spectra were collected in order to check the persistence of the dyes after different exposure times to visible light. As reported in ESI (Figure S2), the presence of the characteristic peaks even after 30 seconds of irradiation confirms that the curing process does not degrade the dye molecules.

Once fixed the most suitable printing parameters in terms of layer thickness and exposition times (see Experimental Section), the production of CAD files enabled the additive manufacturing of several 3D objects (Figure 1c), ranging from 3D microcantilevers to honeycomb structures or actuators (Figure 1d).

Flat specimens were also prepared by DLP printing to perform tensile tests in order to investigate the effect of light irradiation on the mechanical properties of azo-contained polymeric matrices according to several formulations (see Experimental Section). Measurements were performed at room temperature (RT) in quasi-static condition (load ramp: 0.1 N/min). An exemplary stress/strain curve for BEDA sample loaded with DR1M is reported in Figure 2a: measurements start in dark conditions. A linear fit of experimental data reveals a Young's Modulus of about 344 MPa (red dashed line). Under laser irradiation, two effects are clearly visible: the sample shows an almost instantaneous expansion (observed as an increase of about 0.3% of the total length) and a decrease of the elastic constant (black dashed line,  $E_{\text{on}}=87$  MPa).

The initial elastic modulus is then recovered when the laser is switched off and a partial restoring of the pristine length is observed. Here, we ascribe the incomplete length restoring to the pulling force that induces plastic deformations in the membrane. The volume variation occurring under illumination of the azopolymer has been largely investigated in the past years, both theoretically and experimentally.<sup>43, 44</sup> A possible explanation of the effect invokes a cyclic isomerization occurring with an irradiation in the visible range, resulting in resonating transition between the two states and a consequent increase of free volume within the polymeric network.<sup>45</sup> Under laser irradiation, the sample shows an almost instantaneous linear expansion (about 0.3% of the total length) and a decrease of the elastic constant (black dashed line,  $E_{\text{light}}=87$  MPa).

**Figure 2.** Quasi-static stress/strain curve for BEDA-DR1M sample in the dark and under laser-irradiation conditions at a room temperature (a) and at 48°C (b). A change in the Young's modulus (fit with dashed lines) is observed.

The initial elastic modulus is then recovered if the excitation laser is switched off. Some linear contraction of the sample is also observed. In BEDA matrix at RT, a photo-softening was measured with both MR and DR1M dye loaded, as reported in Table 1. This behaviour was largely investigated in the past years, both theoretically and experimentally.<sup>43, 44</sup> A possible explanation of the effect invokes a cyclic isomerization occurring with an irradiation in the visible range, resulting in resonating transition between the two states and a consequent increase of free volume within the polymeric network.<sup>45</sup> Using a polymeric matrix like the one formed by BEDA, thus in glassy state at RT, the transition between trans and cis isomers occurs with the azobenzene groups "frozen" in their position, because of a low mobility. This effect leads to a local change of free volume and thus to an unconstrained chain movement and a decrease of the Young's modulus. When BEMA samples were tested, an opposite behaviour was observed (see data in Table 1) and a photo-hardening was measured. Rubbery matrices show a higher mobility, thus allowing

the azobenzene molecules to migrate through the polymer matrix during the photo-switching. As a consequence, the chain mobility is hindered, and the elastic modulus increased. This tendency was already observed under UV irradiation,<sup>46</sup> but to the best of our knowledge this is the first case in which it is observed under visible light irradiation. Interesting to observe that at higher temperature (48°), in the region of the glass transition temperature, BEDA-DR1M samples exhibit a photo-hardening behavior upon laser irradiation (Figure 2b), in analogy to BEMA. Additional experiments are under consideration to better clarify the mechanical behaviour of these materials. Dynamo-mechanical experiments performed on the same samples confirms these results (see Figure S3). Worth to underline that no changes on the mechanical properties were observed on neat matrices when irradiated with laser light (see ESI Figure S4), thus confirming the fundamental light-responsivity of azo compounds. Thus we can conclude that it is possible to tune the photo-mechanical response of a material from photo-softening to photo-hardening by changing the operational temperature or tuning the matrix composition by properly selecting the  $T_g$  of the matrix.<sup>41</sup>

BEDA-DR1M microcantilevers 2000  $\mu\text{m}$  long, 600  $\mu\text{m}$  wide and 100  $\mu\text{m}$  thick were printed (see Figure 3c for an illustrative picture) in order to highlight the variation of elastic modulus induced into a microstructure upon illumination with the excitation laser beam. The laser beam was slightly focused so that the diameter was as large as the cantilever width and thus approximately one third of the cantilever length. It must be pointed out here that the laser absorption within the cantilever should be taken into account, since it would provide an inhomogeneous intensity profile along the thickness of the cantilever. From the UV-VIS spectra we estimated an absorption coefficient for the BEDA-DR1M as high as 9.597  $\text{mm}^{-1}$  at 532 nm, resulting in about 60% of laser light absorbed within the cantilever. At dark, the microcantilever exhibits a fundamental resonance frequency about 3700 Hz and a corresponding Q factor of 15. Once the laser is switched on, the resonance frequency peak promptly shifts to lower values, because of the photo-softening of the cantilever induced as explained above. At the same time, the photo-softening effect produces an increase of the internal damping and thus a decrease of the quality factor, till the resonance peak cannot be detected anymore. The resonance frequency drop is very fast and after 7 seconds the resonance peak cannot be detected, being totally overwhelmed by the measurement noise. In the specific case, reported in Figure 3, the laser was focused on the constrained end of the suspended beam, as it represents the point where the variation of elastic modulus would have the most relevant impact on the cantilever resonance frequency. Figure S5 in ESI shows that focusing the laser in other locations such as the middle or the tip of the microcantilever would affect less the light-induced change of the fundamental resonance frequency.

**Table 1.** Summary of Young's modulus estimations from quasi-static stress/strain curves for different azopolymer-loaded compounds. Curves for all polymer formulations are reported in ESI, Figure S4.

Sample	$T_g$ [°C]	$T_{\text{operation}}$ [°C]	Young's modulus [MPa] Light off	Young's modulus [MPa] Light on
--------	---------------	--------------------------------	---------------------------------------	--------------------------------------

BEMA	-39	25	22.4	22.4
BEMA-MR	-38	25	5.31	6.14 (+18%)
BEMA-DR1M	-38	25	1.98	3.13 (+58%)
BEDA	39	25	260	260
BEDA	39	48	15	15
BEDA-MR	50	25	260	190 (-27%)
BEDA-DR1M	46	25	343.72	86.85 (-75%)
BEDA-DR1M	46	48	6.8	63 (+620%)

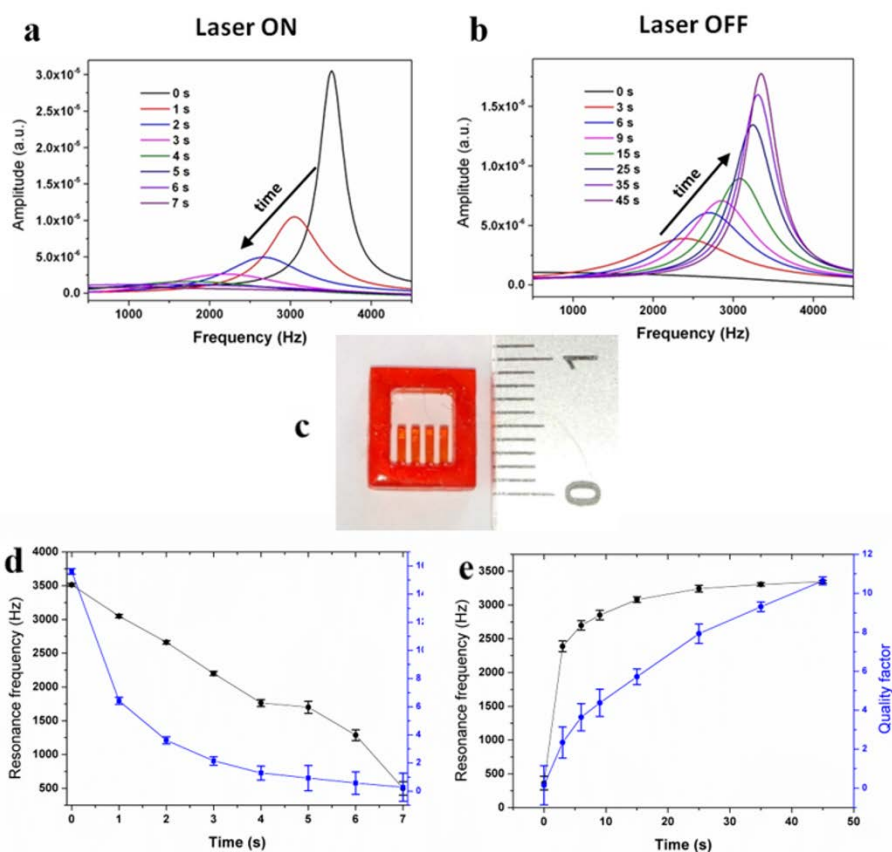


**Figure 3.** Time-evolution of fundamental resonance frequency peak of a BEDA-DR1M printed cantilever at room temperature: switching ON (a) and OFF (b) the laser. c) Photo of the 3D printed microcantilever array. d, e) Time-evolution of resonance frequency and quality factor of the printed microcantilever switching ON (d) and OFF (e) the laser.

When the laser is turned off, an increase of the elastic modulus of the polymer and thus a photo-hardening of the microcantilever is expected. As a consequence, an increase of both resonance

frequency and quality factor of the microcantilever is observed (Figure 3b). With respect to the variation induced by laser irradiation described before, the transition taking place by switching off the

laser is much slower. The fundamental resonance frequency peak needs almost one minute to return in the conditions before the laser illumination.

## Conclusions

In conclusion, we applied a novel approach for developing functional 3D printable materials suitable for DLP printers, exploiting the use of photoactive dyes (i.e. molecules bearing azobenzene moieties) that were used both to produce precise 3D printed structures and to give light triggerable and reversible mechanical response. In fact, upon laser irradiation, the 3D printed structures showed a change in the Young's modulus, resulting in a softening or a hardening depending on the  $T_g$  of the polymeric matrix and the operational temperature. Microcantilevers were produced in a single 3D printing step, showing that this light induced change of mechanical properties could be locally controlled, modifying the features of the printed structure.

## Experimental Section

**Materials** The photocurable monomers Bisphenol A Ethoxylate (2 EO/phenol) diacrylate (Mw 572, BEDA) and Bisphenol A Ethoxylate (15 EO/phenol) dimethacrylate (Mw 1700, BEMA) were purchased from Sigma Aldrich and used as received. 2-(4-Dimethylaminophenylazo) benzoic acid (Methyl Red, MR, Sigma Aldrich) and Disperse Red 1 Methacrylate (DR1M, Sigma Aldrich) were used as photoactive dyes. Irgacure 819 (gently provided by BASF) was used as photoinitiator.

**Sample preparation.** 3D printable formulations were prepared by directly dispersing the dye (either MR or DR1M) in liquid monomers (0.2 per hundred resins, phr) and sonicating for 30 minutes. Then, Irgacure 819 previously dissolved in acetone (amount of Irgacure 2 phr, concentration in acetone 80 mg/ml), was added in each sample. The obtained formulations were then sonicated for additional 30 minutes.

An Asiga Freeform Pico Plus 39 DLP printer using a LED light source (405nm) with an intensity of 22 mW/cm<sup>2</sup> was used for printing (build area: 50 x 31.2 x 76mm, XY resolutions: 39  $\mu$ m, layer thickness is adjustable from 10 to 100  $\mu$ m); the layer exposure time was set at 1.4 s, layer thickness 20  $\mu$ m. A 2 min post curing process was performed with a medium pressure mercury lamp (provided by Robot Factory). The digital models of structures were designed and converted to STL file format for 3D printing. ~~For quasi-static stress/strain measurements, membranes have been employed having dimensions.....~~

**Characterization** The polymerization kinetics was evaluated using an Anton Paar rheometer (Physica MCR 302) with a 25 mm parallel plates geometry equipped with a UV curing set-up that includes a quartz bottom plate and a Hamamatsu LC8 lamp with visible bulb and cut-off filter below 400 nm equipped with 8 mm light guide (Intensity 10mW/cm<sup>2</sup>). All the measurements were performed in isothermal conditions at 25°C and the distance between the two plates was set

at 0,1mm. Oscillatory tests at constant frequency (10 Hz) were conducted within the LVE (0,2%) according to the preliminary amplitude sweep tests; light was turned on after 2 minutes in order to stabilize the system. The variation of storage ( $G'$ ) and loss ( $G''$ ) shear moduli during irradiation was measured as a function of exposure time.

The glass transition temperature ( $T_g$ ) of the materials was evaluated with a Netzsch DSC 204 F1 Phoenix instrument, equipped with a low temperature probe. Samples were put in aluminum pans, BEMA samples were cooled down to -80°C and then heated up to 40 °C while BEDA samples were cooled down to -20°C and heated up to 100 °C (rate: 10 °C min<sup>-1</sup>). For each sample, the same heating cycle was applied two times, the second heating ramp was considered for the evaluation of the  $T_g$ .

Tensile tests were carried out using a Triton Technology TTDMA, testing printed samples (20x10x0.3 mm) in the range 0-5 N with a step of 0.1 N/min. The same equipment was used in dynamo-mechanical configuration (frequency 1 Hz, strain 0.02 mm, T=25°C). A continuous wave laser beam (doubled-frequency Nd:YAG source, emission wavelength  $\lambda$ =532nm, max power 250 mW) has been used for illuminating the sample (Figure S6 in ESI). The beam shows a gaussian profile and has been expanded by a lens so that the illumination spot on the sample is about 1 cm in diameter, resulting in an average density power of 80 mW/cm<sup>2</sup>.

Vibrational analysis of 3D printed cantilevers were performed with a Laser Doppler Vibrometer system (MSA-500, Polytec GmbH). The samples were attached with an adhesive tape on a piezoelectric disk actuator. To analyze the light responsivity of the polymeric structures the excitation laser beam was slightly focused to a diameter of approximately one third of the cantilever length and pointed at different locations along the cantilever length (namely at the constrain point, in the middle and at the end of the cantilever).

## Author Contributions

The manuscript was written through contributions of all authors. All authors have given approval to the final version of the manuscript.

## Funding Sources

This research has received funding from the Italian Flagship Project NANOMAX (Progetto Bandiera MIUR PNR 2011–2013), the Italian FIRB 2011 NEWTON (RBAP11BYNP).

## References

1. T. A. Campbell and O. S. Ivanova, *Nano Today*, 2013, **8**, 119-120.
2. A. Uriondo, M. Esperon-Miguez and S. Perinpanayagam, *Proceedings of the Institution of Mechanical Engineers*,

- Part G: *Journal of Aerospace Engineering*, 2015, **229**, 2132-2147.
3. M. H. Elahinia, M. Hashemi, M. Tabesh and S. B. Bhaduri, *Progress in Materials Science*, 2012, **57**, 911-946.
  4. S. V. Murphy and A. Atala, *Nature Biotechnology*, 2014, **32**, 773-785.
  5. S. Bose, S. Vahabzadeh and A. Bandyopadhyay, *Materials Today*, 2013, **16**, 496-504.
  6. Y. S. Rim, S. H. Bae, H. Chen, N. De Marco and Y. Yang, *Advanced Materials*, 2016, **28**, 4415-4440.
  7. J. A. Lewis and B. Y. Ahn, *Nature*, 2015, **518**, 42-43.
  8. M. Guvendiren, J. Molde, R. M. D. Soares and J. Kohn, *ACS Biomaterials Science and Engineering*, 2016, **2**, 1679-1693.
  9. S. C. Ligon-Auer, M. Schwentenwein, C. Gorsche, J. Stampfl and R. Liska, *Polymer Chemistry*, 2016, **7**, 257-286.
  10. D. Kokkinis, M. Schaffner and A. R. Studart, *Nature Communications*, 2015, **6**, 8643.
  11. A. I. Shallan, P. Smejkal, M. Corban, R. M. Guijt and M. C. Breadmore, *Analytical Chemistry*, 2014, **86**, 3124-3130.
  12. K. B. Anderson, S. Y. Lockwood, R. S. Martin and D. M. Spence, *Analytical Chemistry*, 2013, **85**, 5622-5626.
  13. M. D. Symes, P. J. Kitson, J. Yan, C. J. Richmond, G. J. T. Cooper, R. W. Bowman, T. Vilbrandt and L. Cronin, *Nat Chem*, 2012, **4**, 349-354.
  14. M. Hofmann, *ACS Macro Letters*, 2014, **3**, 382-386.
  15. B. C. Gross, J. L. Erkal, S. Y. Lockwood, C. Chen and D. M. Spence, *Analytical Chemistry*, 2014, **86**, 3240-3253.
  16. M. P. Lee, G. J. T. Cooper, T. Hinkley, G. M. Gibson, M. J. Padgett and L. Cronin, *Scientific Reports*, 2015, **5**, 9875.
  17. J. J. Martin, B. E. Fiore and R. M. Erb, *Nature Communications*, 2015, **6**, 8641.
  18. A. Chiappone, E. Fantino, I. Roppolo, M. Lorusso, D. Manfredi, P. Fino, C. F. Pirri and F. Calignano, *ACS Applied Materials & Interfaces*, 2016, **8**, 5627-5633.
  19. E. Fantino, A. Chiappone, F. Calignano, M. Fontana, F. Pirri and I. Roppolo, *Materials*, 2016, **9**.
  20. D. Lin, Q. Nian, B. Deng, S. Jin, Y. Hu, W. Wang and G. J. Cheng, *ACS Nano*, 2014, **8**, 9710-9715.
  21. M. Vaezi, H. Seitz and S. Yang, *The International Journal of Advanced Manufacturing Technology*, 2013, **67**, 1721-1754.
  22. A. Vitale and T. J. Cabral, *Materials*, 2016, **9**.
  23. E. Fantino, A. Chiappone, I. Roppolo, D. Manfredi, R. Bongiovanni, C. F. Pirri and F. Calignano, *Advanced Materials*, 2016, **28**, 3712-3717.
  24. H. Zeng, P. Wasylczyk, C. Parmeggiani, D. Martella, M. Buresi and D. S. Wiersma, *Advanced Materials*, 2015, **27**, 3883-3887.
  25. M. Irie, T. Fukaminato, K. Matsuda and S. Kobatake, *Chemical Reviews*, 2014, **114**, 12174-12277.
  26. H. Yu, *Journal of Materials Chemistry C*, 2014, **2**, 3047-3054.
  27. N. Hurduc, B. C. Donose, A. Macovei, C. Paius, C. Ibanescu, D. Scutaru, M. Hamel, N. Branza-Nichita and L. Rocha, *Soft Matter*, 2014, **10**, 4640-4647.
  28. X. Ye and M. G. Kuzyk, *Optics Communications*, 2014, **312**, 210-215.
  29. A. M. Rosales, K. M. Mabry, E. M. Nehls and K. S. Anseth, *Biomacromolecules*, 2015, **16**, 798-806.
  30. F. Lagugné Labarthe, T. Buffeteau and C. Sourisseau, *Journal of Physical Chemistry B*, 1999, **103**, 6690-6699.
  31. S. Lee, H. S. Kang, A. Ambrosio, J. K. Park and L. Marrucci, *ACS Applied Materials and Interfaces*, 2015, **7**, 8209-8217.
  32. S. Lee, H. S. Kang and J. K. Park, *Advanced Functional Materials*, 2011, **21**, 1770-1778.
  33. P. Karageorgiev, D. Neher, B. Schulz, B. Stiller, U. Pietsch, M. Giersig and L. Brehmer, *Nature Materials*, 2005, **4**, 699-703.
  34. Z. Mahimwalla, K. G. Yager, J.-i. Mamiya, A. Shishido, A. Priimagi and C. J. Barrett, *Polymer Bulletin*, 2012, **69**, 967-1006.
  35. X. Zhou, Y. Du and X. Wang, *ACS Macro Letters*, 2016, **5**, 234-237.
  36. J. Bin and W. S. Oates, *Scientific Reports*, 2015, **5**.
  37. H. Galinski, A. Ambrosio, P. Maddalena, I. Schenker, R. Spolenak and F. Capasso, *Proceedings of the National Academy of Sciences of the United States of America*, 2014, **111**, 17017-17022.
  38. N. S. Yadavalli, S. Loebner, T. Papke, E. Sava, N. Hurduc and S. Santer, *Soft Matter*, 2016, **12**, 2593-2603.
  39. A. Shimamura, A. Priimagi, J. I. Mamiya, T. Ikeda, Y. Yu, C. J. Barrett and A. Shishido, *ACS Applied Materials and Interfaces*, 2011, **3**, 4190-4196.
  40. H. Zeng, D. Martella, P. Wasylczyk, G. Cerretti, J.-C. G. Lavocat, C.-H. Ho, C. Parmeggiani and D. S. Wiersma, *Advanced Materials*, 2014, **26**, 2319-2322.
  41. I. Roppolo, E. Celasco, M. Sangermano, A. Garcia, T. Gacoin, J. P. Boilot and S. Perruchas, *Journal of Materials Chemistry C*, 2013, **1**, 5725-5732.
  42. D. Iqbal and M. H. Samiullah, *Materials*, 2013, **6**, 116-142.
  43. M. Saphiannikova, V. Toshchevnikov and J. Illynskiy, *Nonlinear Optics Quantum Optics*, 2010, **41**, 27-57.
  44. L. Sorelli, F. Fabbri, J. Frech-Baronet, A.-D. Vu, M. Fafard, T. Gacoin, K. Lahlil, L. Martinelli, Y. Lassailly and J. Peretti, *Journal of Materials Chemistry C*, 2015, **3**, 11055-11065.
  45. H. K. Kim, X. S. Wang, Y. Fujita, A. Sudo, H. Nishida, M. Fujii and T. Endo, *Macromolecular Chemistry and Physics*, 2005, **206**, 2106-2111.
  46. A. Richter, M. Nowicki and B. Wolf, *Molecular Crystals and Liquid Crystals*, 2008, **483**, 49-61.